

Molecules with All Triple Bonds: OCBBCO, N₂BBN₂, and [OB[−]BB[−]BO]^{2−}†

Lucas C. Ducati, Nozomi Takagi, and Gernot Frenking*

Fachbereich Chemie, Philipps-Universität Marburg, Hans-Meerwein-Strasse, D-35043 Marburg, Germany

Received: March 27, 2009; Revised Manuscript Received: June 16, 2009

DFT calculations at the BP86/TZ2P level have been carried out for the compounds OCBBCO, N₂BBN₂, and [OB[−]BB[−]BO]^{2−}. The calculations predict very short distances and large bond dissociation energies for the central B–B bonds. The nature of the bonding situation was investigated with an energy decomposition analysis. It shows that the central boron–boron bonds are genuine triple bonds. The π -bonding contributes between 38–40% to the total orbital interactions of the B \equiv B bonds. The compounds can be considered as donor–acceptor complexes L \rightarrow BB \leftarrow L between the central B₂ moiety in the third [(3)¹ Σ_g^+] excited state and the ligands L = CO, N₂, BO[−]. The π -backdonation L \leftarrow BB \rightarrow L for L = CO, N₂ is very strong, which suggests that the latter bonds should also be considered as triple bonds. The π -bonding in [OB[−]BB[−]BO]^{2−} is weaker, which makes the latter bonds borderline cases for triple bonds. The triple-bond character explains the very large bond dissociation energies for the LB–BL and L–BB–L bonds.

Introduction

Molecules which have homoatomic triple bonds between atoms of the first octal row have until recently been limited to alkynes RC \equiv CR and N₂. In 2002, Zhou and co-workers isolated the compound OCBBCO, which was produced by decomposition of laser vaporized boron atoms with CO in an argon matrix at 8 K.¹ The authors reported also about CASSCF and B3LYP calculations which showed that the ¹ Σ_g^+ singlet state of linear OCBBCO is the electronic ground state which is 20.5 kcal mol^{−1} lower in energy than the ³ Σ_g^- triplet state. The compound OCBBCO was calculated with a very short B–B bond (1.453 Å) and a very large bond dissociation energy $D_e = 143.5$ kcal mol^{−1}. The bond is much shorter and stronger than the calculated B–B double bond in HB=BH (1.507 Å and 113.0 kcal mol^{−1}) which has a ³ Σ_g^- ground state. The calculated bond length and bond dissociation energy and the inspection of the shape of the highest-lying valence orbitals let the authors suggest that OCBBCO “exhibits some boron–born triple bond character.”¹ They also proposed that the Lewis structure of the molecule should be drawn as O=C–B \equiv B–C=O.

A very careful theoretical study of the electronic structure of molecules LBBL with L = CO, CS, N₂, Ar, and Kr using CCSD(T) in conjunction with large basis sets was published by Mavridis et al. in 2004.² They found that the bonding situation in all compounds can be understood in terms of donor–acceptor interactions between two L species that serve as donor ligands and B₂ as acceptor moiety. The B₂ fragment in L \rightarrow BB \leftarrow L is in the third excited (3)¹ Σ_g^+ state that has the valence electron configuration (2 σ_g)²(1 π_u)⁴ where the σ - and the degenerate π -bond are fully occupied yielding a B \equiv B fragment (Figure 1). The bond dissociation energy (BDE) for the B–B bond in LBBL was calculated at the CCSD(T)/QZ level between $D_e = 137.5$ kcal/mol (L = CS) and $D_e = 161.8$ kcal/mol (L = Kr). Very large values were also calculated for the L–BB–L donor–acceptor bonds. The theoretically predicted BDE for dissociation into B₂[(3)¹ Σ_g^+] and 2 ligands L amounts to 226.6 kcal/mol for L = CO and 171.5 kcal/mol for

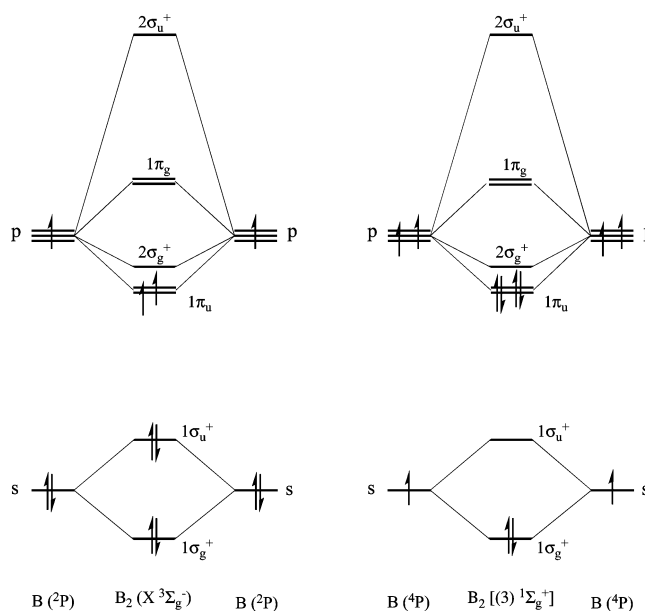


Figure 1. Schematic representation of the X ³ Σ_g^+ ground state and the third excited (3)¹ Σ_g^+ state of B₂.

L = N₂.² This raises the question about the strength of the σ - and π -contributions to the L \rightarrow BB \leftarrow L donor–acceptor bonds. A remarkable feature of the LBBL molecules is that, according to a Mulliken population analysis, the boron atom carries always a small negative partial charge even when it is bonded to the more electronegative nitrogen atoms in N₂BBN₂.

Recently, Li and co-workers observed the boron compound [OB[−]BB[−]BO][−] in the gas phase using photoelectron spectroscopy.³ Quantum chemical calculations using B3LYP, B3PW91, and MP2 were reported for neutral (³ Σ_g^-) OB[−]BB[−]BO, anionic (² Π_u) [OB[−]BB[−]BO][−], and dianionic (¹ Σ_g^+) [OB[−]BB[−]BO]^{2−} molecules in the respective ground states. The latter species is isoelectronic with OCBBCO and N₂BBN₂. The calculation of the bond orders and inspection of the molecular orbitals let the authors suggest that the bonding situation in (¹ Σ_g^+) [OB[−]BB[−]BO]^{2−} is similar to that in OCBBCO and that the dianion has a true B \equiv B triple bond.³

† Part of the “Walter Thiel Festschrift”.

* To whom correspondence should be addressed.

Several questions remain to be answered about the nature of the bonding in the isoelectronic compounds OCBBCO, N₂BBN₂ and [OB BBBBO]²⁻. A central issue concerns the strength of the σ - and π -orbital interactions in the B \equiv B triple bond and a comparison with the C \equiv C and N \equiv N triple bond. In order to address the question, we carried out an energy decomposition analysis (EDA) of the three molecules. We extended the investigation to the donor–acceptor bonds between the B₂ moieties in the third excited (3)¹ Σ_g^+ state and the ligands CO, N₂, BO⁻. The EDA method which was developed by Morokuma⁴ and by Ziegler and Rauk⁵ has been proven to give detailed insight into the nature of the chemical bond in terms of orbital interactions, electrostatic (Coulomb) attraction, and exchange (Pauli) repulsion.⁶ The most important details of the EDA are described in Methods.

Methods

The geometries of the molecules have been optimized using BP86 density functional⁷ in conjunction with TZ2P basis sets.⁸ All structures were verified as minima on the potential energy surface by calculating the Hessian matrices. The calculations were carried out using the ADF program package.⁹

For the calculations of the vibrational frequencies and NBO analyses, we performed BP86 calculations with a def2-TZVPP basis set¹⁰ using BP86/def2-TZVPP optimized geometries that are very similar to the BP86/TZ2P structures. The latter calculations were performed with GAUSSIAN 03.¹¹

The focus of the energy decomposition analysis is the instantaneous interaction energy ΔE_{int} , which is the energy difference between the molecule and the fragments in the frozen geometry of the compound. The interaction energy can be divided into three main components

$$\Delta E_{\text{int}} = \Delta E_{\text{elstat}} + \Delta E_{\text{Pauli}} + \Delta E_{\text{orb}} \quad (1)$$

ΔE_{elstat} gives the electrostatic interaction energy between the fragments, which are calculated using the frozen electron density distribution of the fragments in the geometry of the molecules. The second term in eq 1, ΔE_{Pauli} , refers to the repulsive interactions between the fragments, which are caused by the fact that two electrons with the same spin cannot occupy the same region in space. ΔE_{Pauli} is calculated by enforcing the Kohn–Sham determinant on the superimposed fragments to obey the Pauli principle by antisymmetrization and renormalization. The stabilizing orbital interaction term, ΔE_{orb} , is calculated in the final step of the energy partitioning analysis when the Kohn–Sham orbitals relax to their optimal form. This term can be further partitioned into contributions by the orbitals belonging to different irreducible representations of the point group of the interacting system. The interaction energy, ΔE_{int} , can be used to calculate the bond dissociation energy, $-D_e$, by adding ΔE_{prep} , which is the energy necessary to promote the fragments from their equilibrium geometry to the geometry in the compounds (eq 2). For technical reasons, the energy decomposition analysis involving open-shell fragments does neglect the spin-polarization in the fragments yielding slightly too stable bonds (in the order of a few kcal/mol per unpaired electron). The bond energies have been corrected for the spin-polarization error ΔE_{corr} , which is given in the tables. Further details of the energy partitioning analysis can be found in the literature.¹²

$$-D_e = \Delta E_{\text{prep}} + \Delta E_{\text{int}} \quad (2)$$

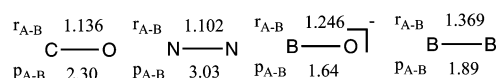
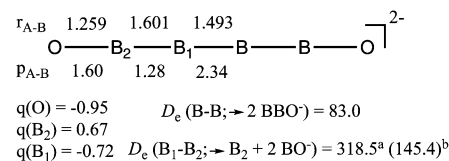
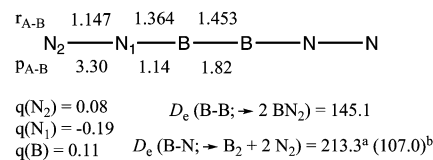
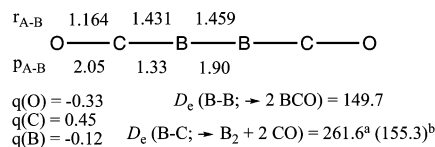


Figure 2. Optimized geometries of OCBBCO, N₂BBN₂ and [OB BBBBO]²⁻ and the diatomic species CO, N₂, BO⁻ and B₂[(3)¹ Σ_g^+] at BP86/TZ2P. Calculated bond length $r_{\text{A-B}}$ [Å], Wiberg bond orders $P_{\text{A-B}}$, atomic partial charges $q(\text{A})$ and bond dissociation energies D_e [kcal/mol]. ^a Dissociation energy with respect to the electronic reference state of B₂, reaction R1. ^b Dissociation energy with respect to the electronic ground state of B₂, reaction R2.

Results and Discussion

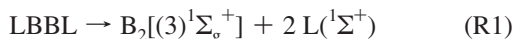
Figure 2 shows the theoretically predicted bond lengths and bond dissociation energies of the calculated molecules at BP86/TZ2P. The atomic partial charges q and the Wiberg bond orders are also given.

The calculated B–B bond lengths of OCBBCO (1.459 Å), N₂BBN₂ (1.453 Å), and [OB BBBBO]²⁻ (1.493 Å) are significantly shorter than the experimental values of typical B–B double bonds which are between 1.57–1.59 Å.¹³ The B–B distances in the three compounds LBBL are also clearly shorter than the theoretical B–B single bond in H₂B–BH₂ (1.623 Å) and the double bond in HB=BH (1.526 Å).¹⁴ Our theoretically predicted B–B distances at BP86/TZ2P for OCBBCO and N₂BBN₂ are in good agreement with the CCSD(T)/QZ values of Mavridis et al. who reported the values 1.439 and 1.460 Å for the two molecules, respectively.² The BP86/TZ2P value for [OB BBBBO]²⁻ is slightly shorter than the MP2/aug-cc-pVTZ value (1.504 Å), which was given by Li and co-workers.³ Figure 2 gives also the calculated equilibrium distances of the free ligands L in the singlet ground state and B₂ in the (3)¹ Σ_g^+ excited state. It becomes obvious that the bond lengths in the ligands L and in B₂[(3)¹ Σ_g^+] become longer in the compounds LBBL.

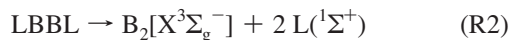
The B–B bond dissociation energies D_e of OCBBCO (149.7 kcal/mol) and N₂BBN₂ (145.1 kcal/mol) at BP86/TZ2P are in good agreement with previous data at the CCSD(T)/QZ level, which are 146.3 and 144.1 kcal mol⁻¹, respectively.² Our calculations suggest that [OB BBBBO]²⁻ has a significantly smaller BDE of $D_e = 83.0$ kcal/mol than the neutral compounds LBBL. We want to point out that there is no correlation between the bond orders P_{BB} , the bond lengths r_{BB} and the BDE of the latter compounds.¹⁹ [OB BBBBO]²⁻ has a only a slightly longer B–B bond than OCBBCO and N₂BBN₂ but the BDE of the dianion is much less while the bond order is much higher ($P_{\text{BB}} = 2.34$) than in OCBBCO ($P_{\text{BB}} = 1.90$) and N₂BBN₂ ($P_{\text{BB}} = 1.82$). The

EDA results given below explain the surprising data. Note that the NBO analysis gives negative partial charges for the central boron atoms in [OB BBBO]²⁻ ($q_{\text{B1}} = -0.72$) and OCBB CO ($q_{\text{B}} = -0.12$) but a small positive charge is calculated for N₂BBN₂ ($q_{\text{B}} = 0.11$). It is remarkable that the central boron atoms in [OB BBBO]²⁻ carry a large negative charge while the boron atoms of the terminal donor moieties carry a large positive charge of $q_{\text{B2}} = 0.67$.

Figure 2 gives also the BDEs for the L→BB←L donor–acceptor bonds. The calculated D_e values for the dissociation into the fragments L in the electronic reference states are very large (reaction 1) (${}^1\Sigma_g^+$ when Y = N₂)



The theoretically predicted reaction energies for reaction 1 suggest that the average BDE for one ligand is 130.8 kcal/mol for L = CO, 106.7 kcal/mol for L = N₂, and 159.3 kcal/mol for L = BO⁻. This is much higher than the D_e values of typical donor–acceptor bonds of main-group Lewis bases that have values of less than 60 kcal/mol.¹⁵ The dissociation of LBBL into the fragments in the electronic ground state is still rather high (reaction 2)



The calculated values given in Figure 2 indicate that the average dissociation energy yielding the B₂[X³Σ_g⁻] ground state is 77.7 kcal/mol for L = CO, 53.5 kcal/mol for L = N₂, and 72.7 kcal/mol for L = BO⁻.

The very large BDEs for reaction 1 let it seem possible that the L→BB←L donor–acceptor bonds have significant contributions from π-bonding. Figure 3 shows the complete sets of occupied valence orbitals of LBBL. The HOMO of all three molecules is the degenerate 2π_u MO, which is the bonding contributions of the p(π) AOs of the central B₂ moiety but it has also large coefficients from the p(π) AOs of the donor atoms of L. The shape of the orbitals clearly indicates that there is substantial π-bonding from B₂ to the ligands L←BB→L. There are two more degenerate valence MOs in LBBL which have π-symmetry. They are the 1π_g MO and the 1π_u MO that are very close in energy (Figure 3). The latter orbitals are the plus and minus combinations of the π-bonding MOs of the ligand fragments L. The remaining seven valence orbitals have σ-symmetry. The strength of the bonding interactions that comes from the σ- and π-orbital to the LB–BL and L–BB–L bonding has been estimated with the EDA calculations. The results are given in Table 1.

The first three entries of the EDA results for LBBL reveal the nature of the LB–BL bonds. The total interaction energies ΔE_{int} are only slightly less than the D_e values because the preparation energies ΔE_{prep} are very small. The breakdown of the ΔE_{int} values into the three energy contributions suggests that the central boron–boron bond in LBBL has a higher covalent than electrostatic character. The attraction which comes from the orbital term ΔE_{orb} is stronger than the electrostatic attraction ΔE_{elstat} (Table 1). The EDA data indicate that there is a significant contribution of the π-orbital interactions to ΔE_{orb} . The calculations show that ΔE_{π} amounts to 37.5–39.7% of the total orbital interactions. This is less than the ΔE_{π} contribution to the orbital interactions in free B₂[(3)¹Σ_g⁺], which has a genuine triple bond, where the π-bonding is nearly as strong as

σ-bonding (Table 2). The EDA results for B₂[(3)¹Σ_g⁺] reveal a very unusual bonding situation which needs to be explained.

The EDA calculations suggest that the electrostatic interactions in B₂[(3)¹Σ_g⁺] are strongly repulsive by 64.4 kcal/mol. The Coulomb interaction in most diatomic molecules is strongly attractive like in N₂ (Table 2). A detailed analysis of the electrostatic and orbital interactions in diatomic molecules shows¹⁶ that the electrostatic repulsion can be explained with the fact that the 2p(σ) AOs of the boron atoms that are the interacting fragments in B₂[(3)¹Σ_g⁺] are empty. A previous EDA analysis of homodiatom molecules E₂ (E = Li–F₂) showed that occupied π-orbitals have repulsive contribution to ΔE_{elstat} . It was also shown that occupied σ-orbitals that come from 2s orbitals are weakly attractive while occupied σ-orbitals that come from p(σ) orbitals have a large stabilizing contribution to ΔE_{elstat} .¹⁶ There is only one occupied valence orbital in the latter molecule that has σ-symmetry while there are two occupied orbitals which have π-symmetry. This explains the unusual finding that the electrostatic term in B₂[(3)¹Σ_g⁺] is repulsive.

The interactions of B₂[(3)¹Σ_g⁺] with the ligands L in OCBB CO, N₂BBN₂, and [OB BBBO]²⁻ yield a significant change in the nature of the boron–boron bond. The EDA calculations suggest that the electrostatic term of the LB–BL bonds is now strongly attractive (Table 1). This can be explained with the σ-donation of the ligands to the B₂ moiety L→BB←L that yields a significant occupation of the vacant 2σ_g⁺ orbital of B₂ (Figure 1). The electrostatic stabilization due to the occupation of the σ-orbital is compensated by a large increase in the Pauli repulsion. Table 1 shows that the ΔE_{Pauli} values for the LB–BL interactions are much higher than for B₂[(3)¹Σ_g⁺] (Table 2).

The π-orbital interactions in B₂[(3)¹Σ_g⁺] yield 47.7% of ΔE_{orb} , which is much higher than the relative contribution of ΔE_{π} in N₂ (34.4%). However, since the percentage contribution of ΔE_{π} in the latter molecule, which has a triple bond, is even slightly less than in the boron–boron bonds of OCBB CO, N₂BBN₂, and [OB BBBO]²⁻, we conclude from the EDA results that the molecules have genuine boron–boron triple bonds even when the relative contributions of ΔE_{π} to the orbital interactions are smaller than in B₂[(3)¹Σ_g⁺]. Our assignment of a boron–boron triple bond is in agreement with previous analyses of the electronic structures of LBBL.^{1–3}

The calculated interaction energies ΔE_{int} and the BDE show (Table 1) that the boron–boron triple bond in [OB BBBO]²⁻ is significantly weaker than in OCBB CO and N₂BBN₂. Intuitively, this might be explained with the release of Coulomb repulsion between the negatively charged fragments [BBO]⁻. The EDA data show that the electrostatic interaction between the latter species at the equilibrium distance of [OB BBBO]²⁻ is strongly attractive with $\Delta E_{\text{elstat}} = -71.0$ kcal/mol. The electrostatic interactions in molecules have been analyzed in a very detailed study, which shows that the partial charges of the interacting fragments should not be used as indicator for the Coulomb interactions.¹⁶ This is because the electronic charge in a molecule has an anisotropic distribution. Partial charges do not give any information about the spacial distribution of the electronic charge that plays a crucial role for the Coulombic interaction. The EDA data suggest that the electrostatic attraction in [OB BBBO]²⁻ is weaker than in OCBB CO and N₂BBN₂ while the attractive orbital interactions ΔE_{orb} in the latter compounds are less than in the dianion. This explains why the bond order of the central B≡B triple bond in [OB BBBO]²⁻ is larger ($P_{\text{BB}} = 2.34$) than in OCBB CO ($P_{\text{BB}} = 1.90$) and N₂BBN₂ ($P_{\text{BB}} = 1.82$). The strength of the B≡B triple bonds in LBBL is not determined by the orbital interactions alone but by the sum of the three

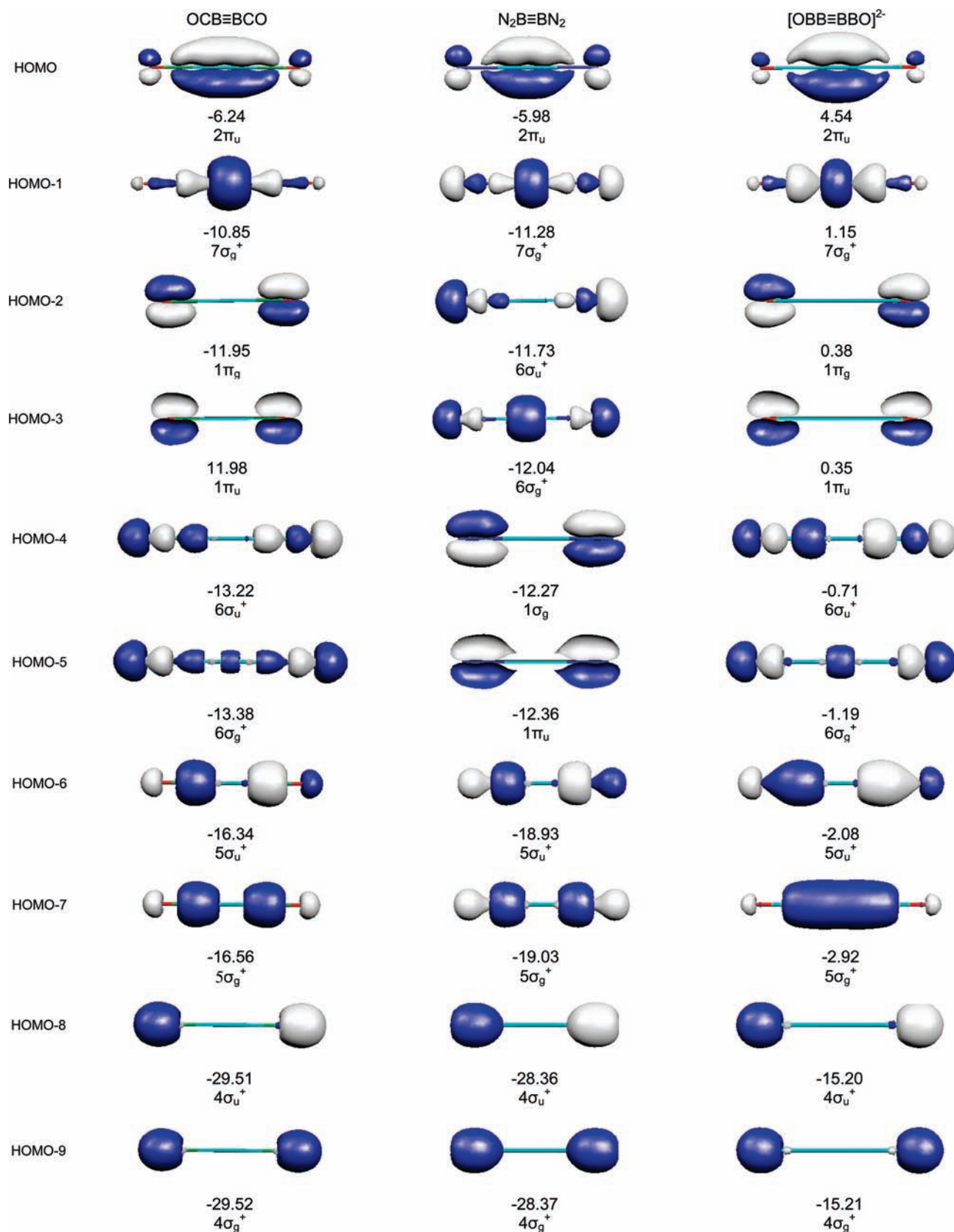


Figure 3. Plot of the occupied valence orbitals of OCBBCO, N₂BBN₂, and [OBBBBO]²⁻.

contributions ΔE_{orb} , ΔE_{elstat} , and ΔE_{Pauli} . Table 1 shows that the main reason for the weaker B≡B triple bond in [OBB-BBO]²⁻ is the much stronger Pauli repulsion. The calculated value for [OBB-BBO]²⁻ is significantly higher ($\Delta E_{\text{Pauli}} = 144.9$ kcal/mol) than for OCBBCO ($\Delta E_{\text{Pauli}} = 103.9$ kcal/mol) and N₂BBN₂

($\Delta E_{\text{Pauli}} = 93.6$ kcal/mol). This is because the exchange (Pauli) repulsion between two electrons that have the same spin is much larger at short distances than Coulombic repulsion.¹⁶

One referee pointed out that the longer and weaker B≡B triple bond in [OBB-BBO]²⁻ may be due to the weaker Coulombic

TABLE 1: EDA Results of L–B≡B–L at the BP86/TZ2P Level^a

	OCB≡BCO	N ₂ B≡BN ₂	[OBB≡BBO] ²⁻	OC–BB–CO	N ₂ –BB–N ₂	[OB–BB–BO] ²⁻
interacting fragments	2 BCO (⁴ Σ ⁻)	2 BNN (⁴ Σ ⁻)	2[BBO] ⁻ (⁴ Σ ⁻)	B ₂ [(3) ¹ Σ _g ⁺] + 2 CO (¹ Σ ⁺)	B ₂ [(3) ¹ Σ _g ⁺] + 2 N ₂ (¹ Σ _g ⁺)	B ₂ [(3) ¹ Σ _g ⁺] + 2 BO ⁻ (¹ Σ ⁺)
ΔE _{int}	-155.2	-155.3	-89.7	-267.7	-223.1	-326.1
ΔE _{Pauli}	103.9	93.6	144.9	203.6	221.3	195.0
ΔE _{elstat} ^b	-108.7 (42.0%)	-97.4 (39.1%)	-71.0 (30.2%)	-119.1 (25.3%)	-94.5 (21.3%)	-209.0 (40.1%)
ΔE _{orb} ^b	-150.4 (58.0%)	-151.5 (60.9%)	-163.6 (69.8%)	-352.2 (74.7%)	-349.9 (78.7%)	-312.2 (59.9%)
ΔE _σ ^c	-92.1 (61.2%)	-91.3 (60.3%)	-102.2 (62.5%)	-193.7 (55.0%)	-168.3 (48.1%)	-233.1 (74.7%)
ΔE _π ^c	-58.3 (38.8%)	-60.2 (39.7%)	-61.4 (37.5%)	-158.5 (45.0%)	-181.6 (51.9%)	-79.1 (25.3%)
ΔE _{prep}	5.5	10.2	6.7	6.1 (112.4) ^d	9.8 (123.1) ^d	7.6 (180.7) ^d
ΔE(= -D _e)	149.7	145.1	83.0	261.6 (155.3) ^d	213.3 (107.0) ^d	318.5 (145.4) ^d

^a Energy values in kcal mol⁻¹. ^b The percentage values in parentheses give the contribution to total attractive interactions ΔE_{orb} + ΔE_{elstat}. ^c The percentage values in parentheses give the contribution to total orbital interactions ΔE_{orb}. ^d Energy with respect to B₂(X³Σ_g⁻) ground state.

TABLE 2: Energy Decomposition Analysis Results of B₂ and N₂ Molecules at BP86/TZ2P Level^a

	N≡N	B≡B[(3) ¹ Σ _g ⁺]
interacting fragments	2 N (⁴ Σ ⁻)	2 B (⁴ Σ ⁻)
ΔE _{int}	-240.3	-127.7
ΔE _{Pauli}	802.4	13.5
ΔE _{elstat} ^b	-312.9 (30.0%)	64.4 (0.0%)
ΔE _{orb} ^b	-729.8 (70.0%)	-205.6 (100.0%)
ΔE _σ ^c	-478.8 (65.6%)	-107.6 (52.3%)
ΔE _π ^c	-251.0 (34.4%)	-98.0 (47.7%)
ΔE _{prep}	4.2 ^e	3.3 ^e (100.4) ^d
ΔE(= -D _e)	236.1	124.4 (27.4) ^d

^a Energy values in kcal mol⁻¹. ^b The percentage values in parentheses give the contribution to total attractive interactions ΔE_{orb} + ΔE_{elstat}. ^c The percentage values in parentheses give the contribution to total orbital interactions ΔE_{orb}. ^d Energy with respect to B(²P) ground state. ^e Correction for spin polarization.

attraction which could be related to the large negative charges at the central boron atoms q(B₁) = -0.72 (Figure 2). The assumption is not correct. EDA calculations of [OBB–BBO]²⁻ where the central boron–boron bond was frozen at shorter distances than the equilibrium value show that the electrostatic attraction becomes stronger even at r(B≡B) = 1.200 Å where ΔE_{elstat} = -102.1 kcal/mol. The reason for the longer equilibrium distance is the steep increase in the Pauli repulsion term when the boron–boron bond becomes shorter.

Table 1 gives also the EDA result for the L–BB–L bonds. Calculations have been performed for the simultaneous interactions between both ligands L and the central B₂. The data show that the average interaction energies for the L–BB–L systems are very large. The calculated values for one B–L bond are ΔE_{int} = -133.9 kcal/mol for OCBBCO, ΔE_{int} = -111.6 kcal/mol for N₂BBN₂, and ΔE_{int} = -163.1 kcal/mol for [OBB–BBO]²⁻. The largest contributions to the interaction energy come from the orbital term ΔE_{orb}. Note that the breakdown of the latter term into σ- and π-orbitals shows that the π-backdonation L←BB→L for L = CO is very large (45.0% of ΔE_{orb}) and even larger for L = N₂ (51.9% of ΔE_{orb}) where it is even bigger than the σ-donation. It is interesting to note that N₂ is a stronger π-acceptor for B₂[(3)¹Σ_g⁺] than CO. The negatively charged ligand [BO]⁻ is as expected a weaker π-acceptor than CO and N₂. Table 1 shows that the π-backdonation L←BB→L for L = BO⁻ is only 25.3% of ΔE_{orb}. The much stronger total interaction energy ΔE_{int} = -326.1 kcal/mol for [OB–BB–BO]²⁻ compared with the neutral systems L–BB–L comes mainly from the significantly larger electrostatic attraction and to a smaller extent from the weaker Pauli repulsion. This holds also for the stronger OC–BB–CO bonds compared with N₂–BB–N₂. The ΔE_{int} value of the former compound is larger and the ΔE_{Pauli} value is smaller than for the latter while the ΔE_{orb} values are

TABLE 3: Calculated IR and Raman Frequencies (cm⁻¹) and Their Intensities (km/mol and Å⁴/amu, Respectively) at BP86/def2-TZVPP//BP86/def2-TZVPP Level; Experimental Values Are Given in Parentheses^a

frequency	vibrational mode	intensity (IR)	intensity (Raman)
O=C–B≡B–C≡O			
217.4	B–B≡B bend ^b		12.0
481.5	B–B stretch		70.5
478.2	B–C stretch		72.1
509.6	O=C–B bend ^b		0.4
514.6 (517.1)	O=C–B bend	10.7	
1069.0 (1086.1)	B–C stretch	26.8	
1658.3	B≡B stretch		0.6
2042.0 (2014.2)	C≡O stretch	2621.5	
2093.3	C≡O stretch		200.5
N≡N–B≡B–N≡N			
266.5	N–B≡B bend ^b		2.6
487.6	N≡N–B bend ^b		8.3
496.5	N≡N–B bend ^b	1.4	
503.7	B–N stretch		70.3
1153.0	B–N stretch	33.4	
1704.2	B≡B stretch		14.8
2018.0	N≡N stretch		419.5
2033.4	N≡N stretch	1485.1	
[O≡B–B≡B–B≡O] ²⁻			
233.4	B–B≡B bend ^b		64.6
403.3	B–B stretch		91.2
478.6	O≡B–B bend ^b		3.6
487.7	O≡B–B bend ^b	33.8	
830.8	B–B stretch	0.6	
1453.9	B≡B stretch		35.5
1682.3	O≡B stretch	2010.4	
1737.5	O≡B stretch		254.4

^a Data from ref 1. ^b Degenerate mode.

not very different from each other. This shows that the differences between bond strengths are sometimes not related to differences between the strengths of orbital interactions.¹⁷ The comparatively small contribution of the π-orbital interaction to the B₁–B₂ bond in [OB–BB–BO]²⁻ show that it is a borderline case for calling it a triple bond.

The calculated values for the σ- and π-orbital interactions of L–BB–L that indicate the relative strength of σ-donor and π-acceptor strength of L may be compared with the overall charge distribution of the B₂ and L₂ moieties. Figure 2 shows that the B₂ fragment in N₂BBN₂ donates 0.22 e to the N₂ ligands while the B₂ moieties in OCBBCO and [OBBBBO]²⁻ accept electronic charge from the ligands. The net charge donation L→BB←L is 0.24 e for L = CO and 0.56 for L = BO⁻. The calculated charge distribution and the strength of the σ- and π-orbital interactions thus suggest that the σ-donor strength has the order BO⁻ > CO > N₂ while the π-acceptor strength has the trend N₂ > CO > BO⁻. The same conclusion was reached for the ligands BO⁻ and CO in a paper by Ehlers et al.²⁰

We calculated the vibrational spectra of the three compounds. The results are given in Table 3. The theoretical infrared and Raman harmonic frequencies at BP86/def2-TZVPP//BP86/def2-TZVPP are in good agreement with the experimental results for OCBBCO. The calculated frequency for the B≡B stretching mode of the LBBL compounds is significantly higher than the experimental stretching mode for diatomic B₂ in its X ³Σ_g⁻ ground state (1051.3 cm⁻¹).¹⁸ Note that the calculated B≡B stretching frequencies of the neutral compounds OCBBCO (1658.3 cm⁻¹) and N₂BBN₂ (1704.2 cm⁻¹) are significantly larger than for [OB⁻BBBO]²⁻ (1453.9 cm⁻¹), which is in agreement with the much weaker B–B interaction energy of the latter molecule (Figure 1).

Summary and Conclusion

The results of this work can be summarized as follows. The energy decomposition analysis of the compounds OCBBCO, N₂BBN₂, and [OB⁻BBBO]²⁻ shows that the central boron–boron bonds are genuine triple bonds. The π-bonding contributes between 38–40% to the total orbital interactions of the B≡B bonds. The compounds can be considered as donor–acceptor complexes L→BB←L between the central B₂ moiety in the third [(3)¹Σ_g⁺] excited state and the ligands L = CO, N₂, BO⁻. The π-backdonation L←BB→L for L = CO, N₂ is very strong, which suggests that the latter bonds should also be considered as triple bonds. The π-bonding in [OB←BB→BO]²⁻ is weaker, which makes the latter bonds borderline cases for triple bonds. The triple-bond character explains the very large bond dissociation energies for the LB–BL and L–BB–L bonds.

Acknowledgment. L.C.D. is grateful to FAPESP (Grant 06/02783-9) for a scholarship. This work was supported by the Deutsche Forschungsgemeinschaft. Excellent service by the computer center (HRZ) of the Philipps-Universität Marburg is gratefully acknowledged.

References and Notes

- (1) Zhou, M.; Tsumori, N.; Li, Z.; Fan, K.; Andrews, L.; Xu, Q. *J. Am. Chem. Soc.* **2002**, *124*, 12936.
- (2) Papakondylis, A.; Miliordos, E.; Mavridis, A. *J. Phys. Chem. A* **2004**, *108*, 4335.
- (3) Li, S.; Zhai, H.; Wang, L. *J. Am. Chem. Soc.* **2008**, *130*, 2573.
- (4) Morokuma, K. *J. Chem. Phys.* **1971**, *55*, 1236.
- (5) Ziegler, T.; Rauk, A. *Theor. Chim. Acta* **1977**, *46*, 1.
- (6) Lein, M.; Frenking, G. In *Theory and Applications of Computational Chemistry: The First 40 Years*; Dykstra, C. E., Frenking, G., Kim, K. S., Scuseria, G. E., Eds.; Elsevier: Amsterdam, 2005; p 291.
- (7) (a) Becke, A. D. *Phys. Rev. A* **1998**, *38*, 3098. (b) Perdew, J. P. *Phys. Rev. B* **1986**, *33*, 8822.
- (8) Snijders, J. G.; Baerends, E. J.; Vernooijs, P. *At. Data Nucl. Data Tables* **1982**, *26*, 483.

(9) Baerends, E. J.; Autschbach, J.; Berces, A.; Bickelhaupt, F. M.; C. Bo, C.; Boerrigter, P. M.; Cavallo, L.; Chong, D. P.; Deng, L.; Dickson, R. M.; Ellis, D. E.; van Faassen, M.; Fischer, L.; Fan, T. H.; Fonseca Guerra, C.; van Gisbergen, S. J. A.; Groeneveld, J. A.; Gritsenko, O. V.; Grüning, M.; Harris, F. E.; van den Hoek, P.; Jacob, C. R.; Jacobsen, H.; Jensen, L.; van Kessel, G.; Kootstra, F.; van Lenthe, E.; McCormack, D. A.; Michalak, A.; Neugebauer, J.; Osinga, V. P.; Patchkovskii, S.; Philipsen, P. H. T.; Post, D.; Pye, C. C.; Ravenek, W.; Ros, P.; Schipper, P. R. T.; Schreckenbach, G.; Snijders, J. G.; Solà, M.; Swart, M.; Swerhone, D.; te Velde, G.; Vernooijs, P.; Versluis, L.; Visscher, L.; Visser, O.; Wang, F.; Wesolowski, T. A.; van Wezenbeek, E.; Wiesenekker, G.; Wolff, S.; Woo, T.; Yakovlev, A.; Ziegler, T. *ADF*, 2006.01, SCM, Theoretical Chemistry, Vrije Universiteit: Amsterdam, The Netherlands. URL: <http://www.scm.com>.

(10) Weigend, F.; Ahlrichs, R. *Phys. Chem. Chem. Phys.* **2005**, *7*, 3297.

(11) Frisch, M. J.; Trucks, G. W.; Schlegel, H. B.; Scuseria, G. E.; Robb, M. A.; Cheeseman, J. R.; Montgomery Jr., J. A.; Vreven, T.; Kudin, K. N.; Burant, J. C.; Millam, J. M.; Iyengar, S. S.; Tomasi, J.; Barone, V.; Mennucci, B.; Cossi, M.; Scalmani, G.; Rega, N.; Petersson, G. A.; Nakatsuji, H.; Hada, M.; Ehara, M.; Toyota, K.; Fukuda, R.; Hasegawa, J.; Ishida, M.; Nakajima, T.; Honda, Y.; Kitao, O.; Nakai, H.; Klene, M.; Li, X.; Knox, J. E.; Hratchian, H. P.; Cross, J. B.; Bakken, V.; Adamo, C.; Jaramillo, J.; Gomperts, R.; Stratmann, R. E.; Yazyev, O.; Austin, A. J.; Cammi, R.; Pomelli, C.; Ochterski, J. W.; Ayala, P. Y.; Morokuma, K.; Voth, G. A.; Salvador, P.; Dannenberg, J. J.; Zakrzewski, V. G.; Dapprich, S.; Daniels, A. D.; Strain, M. C.; Farkas, O.; Malick, D. K.; Rabuck, A. D.; Raghavachari, K.; Foresman, J. B.; Ortiz, J. V.; Cui, Q.; Baboul, A. G.; Clifford, S.; Cioslowski, J.; Stefanov, B. B.; Liu, G.; Liashenko, A.; Piskorz, P.; Komaromi, I.; Martin, R. L.; Fox, D. J.; Keith, T.; Al-Laham, M. A.; Peng, C. Y.; Nanayakkara, A.; Challacombe, M.; Gill, P. M. W.; Johnson, B.; Chen, W.; Wong, M. W.; Gonzalez, C.; Pople, J. A. *Gaussian 03*, rev. D.01; Gaussian, Inc.: Wallingford, CT, 2004.

(12) (a) Bickelhaupt, F. M.; Baerends, E. J. *Rev. Comp. Chem.* **2000**, *15*, 1. (b) Te Velde, G.; Bickelhaupt, F. M.; Baerends, E. J.; Fonseca Guerra, C.; Van Gisbergen, J. A.; Snijders, J.; Ziegler, T. *J. Comput. Chem.* **2001**, *22*, 931.

(13) North, H.; Knizek, J.; Ponikvar, W. *J. Inorg. Chem.* **1999**, *11*, 1931.

(14) Kovács, A.; Esterhuysen, C.; Frenking, G. *Chem.—Eur. J.* **2005**, *11*, 1813.

(15) Jonas, V.; Frenking, G.; Reetz, M. T. *J. Am. Chem. Soc.* **1994**, *116*, 8741.

(16) Krapp, A.; Bickelhaupt, F. M.; Frenking, G. *Chem.—Eur. J.* **2006**, *12*, 9196.

(17) The same explanation was given for the different bond strengths of the ligands PCl₃ and PMe₃ in transition metal complexes. See Frenking, G.; Wichmann, K.; Fröhlich, N.; Grobe, J.; Golla, W.; Le Van, D.; Krebs, B.; Läge, M. *Organometallics* **2002**, *21*, 2921.

(18) Huber, K. P.; Herzberg, G. *Molecular Spectra and Molecular Structure. IV. Constants of Diatomic Molecules*; Van Nostrand Reinhold Co.: New York, 1979.

(19) One referee pointed out that the concept of bond order, which is connected to covalent bonding, should be fundamentally related to the orbital interaction term ΔE_{orb}. The data in Figure 2 and Table 1 show that this is not the case even when values for the same type of bond are compared with each other. For example, the central B≡B bond in N₂BBN₂ has a smaller P_{A–B} value of 1.82 than in OCBBCO (P_{A–B} = 1.90) but the orbital interactions for the boron–boron bond in the latter molecule are slightly weaker (ΔE_{orb} = –150.4 kcal/mol) than in the former species (ΔE_{orb} = –151.5 kcal/mol).

(20) Ehlers, A. W.; Baerends, E. J.; Bickelhaupt, F. M.; Radius, U. *Chem.—Eur. J.* **1998**, *4*, 210.

JP902780T